Semiconductor Physics, Quantum Electronics & Optoelectronics, 2015. V. 18, N 3. P. 248-254.
doi: 10.15407/spqeo18.03.248

PACS 64.70.pn, 78.67.-n, 82.80.Gk

Annealing-induced formation of $Sn_2P_2S_6$ crystallites in As_2S_3-based glass matrix

Yu.M. Azhniuk[1], A.V. Gomonnai[1], O.O. Gomonnai[2], S.M. Hasynets[3], F. Kováč[4], V.V. Lopushansky[1], I. Petryshynets[4], V.M. Rubish[3], D.R.T. Zahn[5]
[1]*Institute of Electron Physics, National Academy of Sciences of Ukraine, 21, Universytetska str., 88017 Uzhhorod, Ukraine*
[2]*Uzhhorod National University, 46, Pidhirna str., 88000 Uzhhorod, Ukraine*
[3]*Uzhhorod Scientific and Technology Center, Institute for Information Recording, National Academy of Sciences of Ukraine, 4, Zamkovi Skhody, 88000 Uzhhorod, Ukraine*
[4]*Institute of Materials Science, Slovak Academy of Sciences, Watsonova 47, Košice 04001, Slovakia*
[5]*Chemnitz University of Technology, D-09107 Chemnitz, Germany*
Phone +38(0312)-643822; fax +38(0312)-643650; e-mail: yu.azhniuk@gmail.com

Abstract. Sn–As–P–S glasses were obtained using co-melting of pre-synthesized As_2S_3 and $Sn_2P_2S_6$. Their structure and composition were confirmed by X-ray diffraction, scanning electron microscopy, energy dispersive X-ray spectroscopy, and micro-Raman scattering. Crystallization of $Sn_2P_2S_6$ crystallites from the glass matrix is observed at annealing under relatively low temperatures (410…580 K).

Keywords: glass, nanostructures, electron microscopy, Raman spectroscopy.

Manuscript received 02.03.15; revised version received 14.05.15; accepted for publication 03.09.15; published online 30.09.15.

1. Introduction

$Sn_2P_2S_6$ (ditin hexathiodiphosphate) is a well-known ferroelectric material that has become an object of extensive theoretical and experimental interest in view of phase transitions and polycritical phenomena observed under variation of temperature and pressure as well as possible applications, in particular for piezo- and pyroelectric gauges and as photorefractive materials [1–4 and references therein]. At ambient pressure, the $Sn_2P_2S_6$ crystal undergoes a second-order structural transition from the ferroelectric phase (*Pn*) to the paraelectric ($P2_1/n$) one at 337 K, which was thoroughly investigated by X-ray diffraction [5], dielectric studies [6], Raman scattering [7-9], inelastic neutron scattering [10], ultrasonic measurements [11], optical spectroscopy [12], birefringence measurements [13], Mössbauer spectroscopy [14, 15], X-ray photoelectron spectroscopy [16, 17], soft X-ray fluorescence spectroscopy [16], and thermal expansion studies [18]. In most cases, these studies were carried out for good quality bulk single crystals.

Much less studied are micro- and nanocrystalline $Sn_2P_2S_6$-based materials. In $Sn_2P_2S_6$ ceramics with grain sizes below 1 μm a decrease of the phase transition temperature by 12 K with respect to the bulk sample was observed in dielectric measurements [19]. Nanocrystalline $Sn_2P_2S_6$ powders with average crystallite sizes down to 20 nm were obtained earlier using soft chemistry (exchange reaction in an aqueous medium)

[20, 21], ball milling from single crystals [22], and ball milling from elemental components with subsequent microwave treatment [23]. Fabrication and investigation of nanoscale ferroelectric materials are important in view of both fundamental and practical aspects. The experience of obtaining nanocrystals in amorphous matrices, especially well known for II-VI chalcogenides (see *e.g.* [24, 25] and references therein), inspired to use such an approach for glass-embedded nanoscale ferroelectric chalcogenide-based materials in order to study size-related effects and possible applications of such systems. In our recent studies, we reported on laser beam annealing-induced formation of SbSI ferroelectric nanocrystals in As_2S_3-based glass matrix [26, 27].

Here, we present scanning electron microscopy (SEM), energy-dispersive X-ray fluorescence spectroscopy (EDX), and Raman scattering studies of Sn–As–P–S system revealing evidence for the formation of $Sn_2P_2S_6$ nanocrystals in the glass matrix upon annealing at relatively low temperatures (below 580 K).

2. Experimental

Sn–As–P–S glasses were prepared by vacuum (~0.01 Pa) co-melting of a mixture of As_2S_3 and $Sn_2P_2S_6$ components both synthesized from high-purity elemental substances. Polycrystalline $Sn_2P_2S_6$ was obtained by cooling a homogenized (for 72 h) melt from 900 K to room temperature. As_2S_3 glass was obtained by cooling a homogenized (for 24 h) melt from 780 K in air. As_2S_3 and $Sn_2P_2S_6$ were co-melted and homogenized at 850–870 K for 24 h with occasional stirring and subsequently hardened in air. Variation of the component ratio enabled a series of $(1–x)As_2S_3{\cdot}xSn_2P_2S_6$ materials with x ranging from 0.1 to 0.43 to be obtained.

Scanning electron microscopy studies combined with energy dispersive X-ray spectroscopy were performed using a SEM JEOL 7000F setup. Micro-Raman measurements were carried out using a Dilor XY800 triple monochromator with a CCD camera and a Kr^+ laser (λ_{exc} = 647.1 nm). Macro-Raman measurements were performed using a LOMO DFS-24 double monochromator with a FEU-136 phototube and a He-Ne laser (λ_{exc} = 632.8 nm). The instrumental resolution was better than 2 cm^{-1}. All the measurements were carried out at room temperature.

3. Results and discussion

Fig. 1 shows SEM scans of the $0.8As_2S_3{\cdot}0.2Sn_2P_2S_6$ sample surface before and after annealing at 442 K. As one can see, the patterns for the annealed samples exhibit higher roughness probably related to some annealing-induced transformation in the material, which can involve phase separation and/or chemical reactions on the surface. The typical size of the inclusions shown in Fig. 1 is below 1 μm.

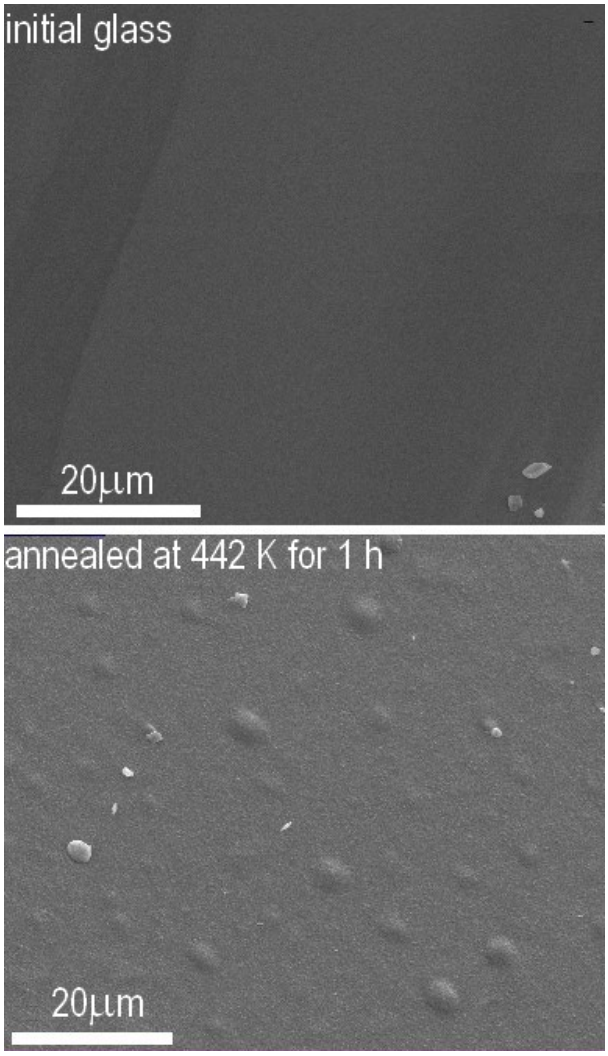

Fig. 1. SEM patterns of $0.8As_2S_3{\cdot}0.2Sn_2P_2S_6$ glass before and after annealing at 442 K for 1 h.

The EDX measurements performed together with SEM (Fig. 2) enabled us to estimate the chemical composition of the samples. It should be mentioned that the EDX data in Fig. 2 differ somewhat from the intended chemical composition (for this sample the chemical formula corresponds to a relative atomic composition of 6.66% Sn, 6.66% P, 26.66% As, and 60.02% S). The EDX data noticeably underestimate the phosphorus content and overestimate that of tin: according to the initial glass composition their values should be equal while the EDX measurements reveal a significant difference. While the sulphur content determined from EDX in the initial glass is close to that in the initial mixture, it somewhat decreases after annealing. A similar trend is observed for other samples (see, for instance, Fig. 3), and this loss of sulphur can be explained by its volatility due to the high vapour pressure.

Raman spectra of as-synthesized $(1–x)As_2S_3{\cdot}xSn_2P_2S_6$ glasses are shown in Fig. 4. The extensively studied Raman spectrum of glassy As_2S_3 [28-37]

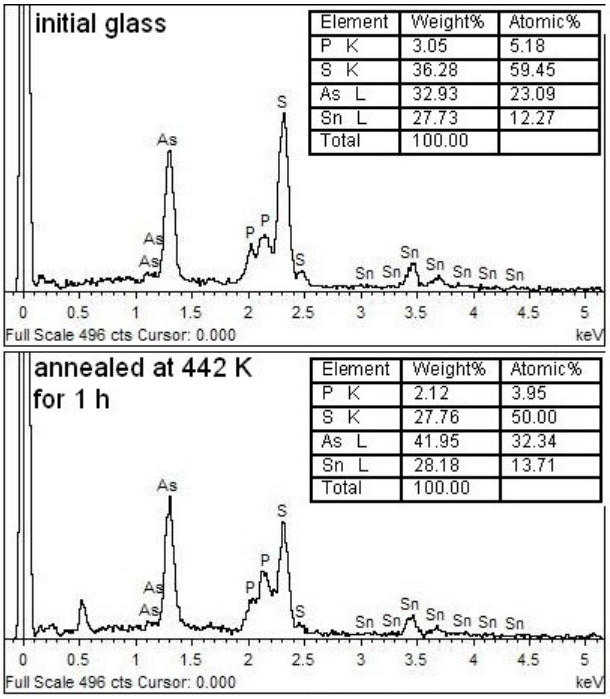

Fig. 2. EDX spectra of $0.8As_2S_3{\cdot}0.2Sn_2P_2S_6$ glass before and after annealing at 442 K for 1 h and the estimated element content in the samples.

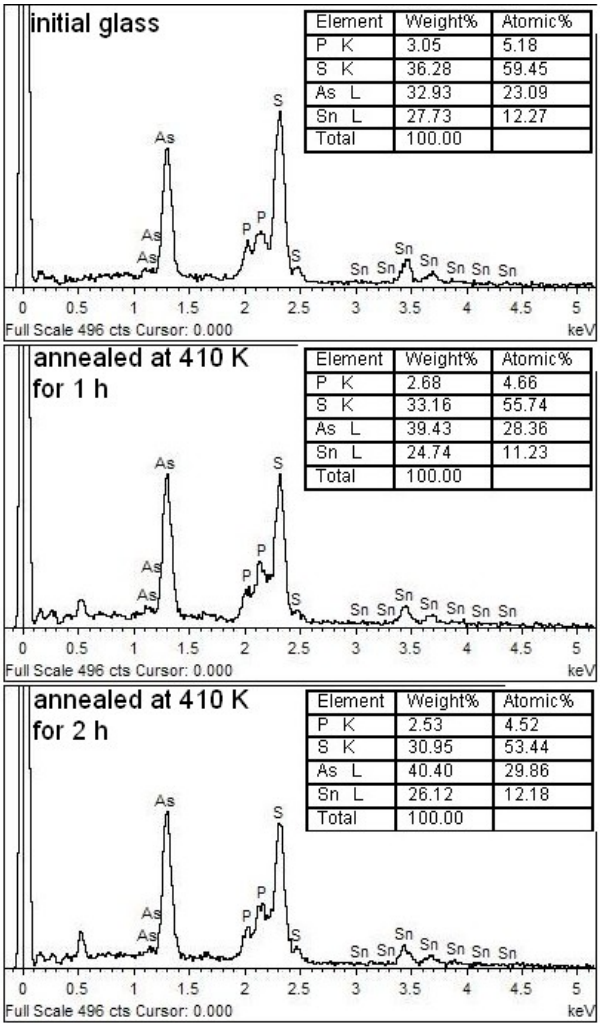

Fig. 3. EDX spectra of $0.8As_2S_3{\cdot}0.2Sn_2P_2S_6$ glass before and after annealing at 410 K and the estimated element content in the samples.

is known to be dominated by a broad band in the range of 300−400 cm^{-1}, which is related to symmetric stretching vibrational modes of $AsS_{3/2}$ pyramids (AsS_3 pyramids are linked together by As–S–As bonds) [31, 33]. A weak band at 490 cm^{-1} is attributed to S–S stretching vibrations in S_8 rings indicating the presence of excessive sulphur [33]. Low-intensity bands centered near 185 and 230 cm^{-1} are ascribed to bending modes of $AsS_{3/2}$ pyramids as well as S_8 and As_4S_4 structural groups that are known to be present in As_2S_3 glass [33–35 and references therein].

With a gradual increase of $Sn_2P_2S_6$ content, the Raman spectra of $(1–x)As_2S_3{\cdot}xSn_2P_2S_6$ glasses are characterized not only by broad features typical for amorphous materials, but also by somewhat narrower bands that can be related to the vibrations of new structural groups. At $x = 0.1$, a shoulder at 408 cm^{-1} appears, it already at $x = 0.2$ becomes a rather narrow peak and with further increase in x develops into the dominant one in the Raman spectrum (Fig. 4). This band is most likely related with formation of new structural groups in the Sn–As–P–S glass structure. Note that for As–P–S glasses similar behaviour was observed: with increasing phosphorus content, a rather narrow band emerged at 418 cm^{-1}, rapidly growing in its intensity [38]. Such a sharp Raman band observed for glassy material is, according to Ref. [38 and references therein], characteristic of an intermediate range order in glasses, usually of a breathing vibration of ring structures. It was assumed that in As–P–S glasses eight-membered $As_2P_2S_4$ rings are formed by sulphur bridges joining $AsS_{3/2}$ pyramids and $S{=}PS_{3/2}$ tetrahedra in the glass structure. The breathing mode of these rings corresponds to the band at 418 cm^{-1} [38]. In our case, the rather close frequency and similar dependence on composition of the band at 408 cm^{-1} suggest the same explanation. The slight difference in frequency can evidently be explained by the different long-range environment somewhat distorting the rings under consideration. It should also be mentioned that in our earlier study of $Sn_2P_2S_6$ nanocrystals obtained by ball milling we observed the weak band centred at 406 cm^{-1}, assumed to stem from partial S→O substitution in PS_3 pyramids due to oxidation at the nanocrystal surface [22]. The band of similar frequency at 411 cm^{-1} was observed in the Raman spectra of $Sn_2P_2S_6$ crystals recovered after high-pressure treatment, where it was possibly related to pressure-induced defects [39]. Still, in the present case, based on the above speculations, we consider the breathing mode of $As_2P_2S_4$ rings in the glass structure to be the most appropriate explanation of the Raman peak in question.

Semiconductor Physics, Quantum Electronics & Optoelectronics, 2015. V. 18, N 3. P. 248-254.
doi: 10.15407/spqeo18.03.248

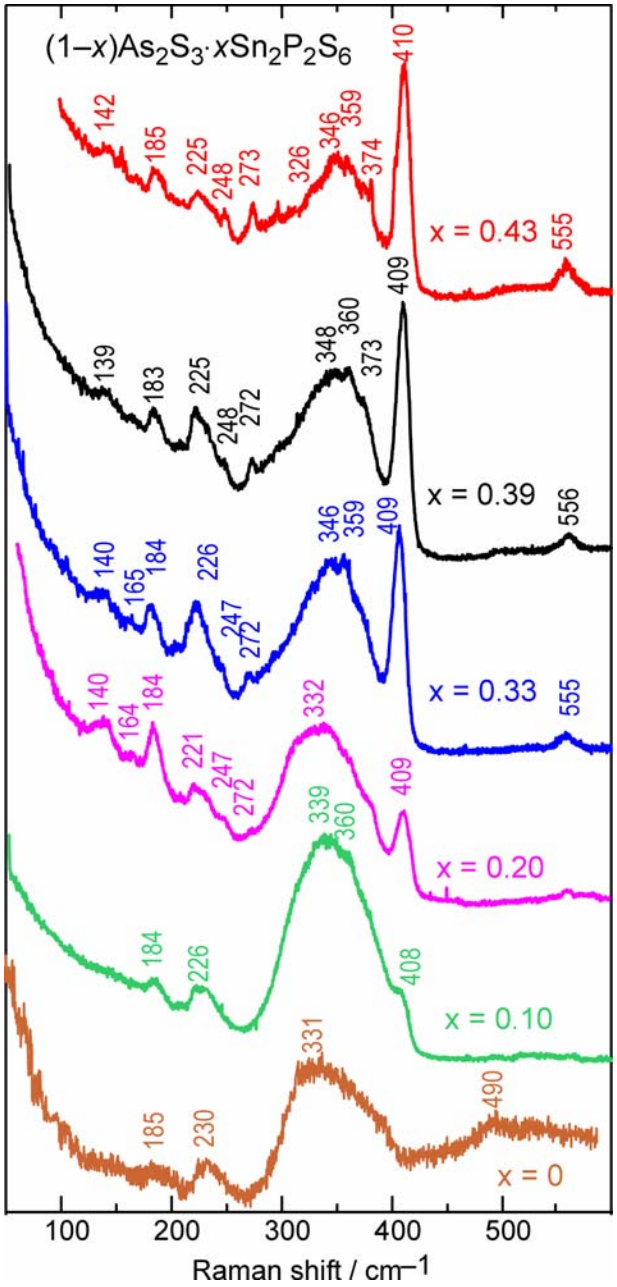

Fig. 4. Raman spectra of unannealed $(1–x)As_2S_3·xSn_2P_2S_6$ glasses.

Simultaneously, the increase of x results in more pronounced features near 185 and 225 cm^{-1} indicating the increasing concentration of S_8 and As_4S_4 structural groups in the glass. Besides, new features near 140, 247, and 272 cm^{-1} appear as evidence for formation of new bonds in the glass. In As–P–S glasses, the increasing phosphorus content also resulted in new Raman bands in the spectra, namely peaks near 150, 230, and 268 cm^{-1}. These were attributed to the vibrational modes of S_8, $S=PS_{3/2}$ (as well as P_4S_7), and P_4S_{10} groups, respectively [38]. With increasing $Sn_2P_2S_6$ content, some structure gradually emerges in the region of the main broad As_2S_3-related band. Similar transformations were observed for As–P–S glasses, where a clear splitting of the band was recorded for $x \geq 0.4$ [38]. There the band emerging at 368 cm^{-1} was ascribed to vibrations of $S=PS_{3/2}$ tetrahedra. In our case, the maximum emerging near 374 cm^{-1} (for $x \approx 0.4$) might be also related to P–P bond vibration, the frequency of which in $Sn_2P_2S_6$ is near 380 cm^{-1} at room temperature [7, 8]. Slightly above 550 cm^{-1}, a rather broad band is observed, which can be related to vibrations of P_2S_6 structural groups present in the basically amorphous network, since it is known that the Raman spectrum of $Sn_2P_2S_6$ contains five bands assigned to internal vibrations of $(P_2S_6)^{4-}$ anions [3]. The splitting related to a crystal environment as well as two-fold Davydov splitting of these bands reported in [3] cannot be resolved in the unpolarized spectra of glass-based composites shown in Fig. 4. In general, the overall appearance of the Raman spectra of the as-synthesized $(1–x)As_2S_3·xSn_2P_2S_6$ samples is consistent with their amorphous structure and the presence of some pronounced structural groups.

Note that the Raman spectrum of the $(1–x)As_2S_3·xSn_2P_2S_6$ glasses does not change with the measurement time indicating the glass stability, contrary to the case of As–Sb–S–I and Tl–In–As–Se glasses, where we recently observed rapid laser beam-induced crystallization of SbSI [26, 27] and $TlInSe_2$ [40] crystallites, respectively.

The changes in the Raman spectra after annealing (Fig. 5) noticeably depend on the glass composition. For the glasses with lower $Sn_2P_2S_6$ content, only slight changes are observed (sharpening of some features and a slight increase of their intensity). Meanwhile, the samples with higher $Sn_2P_2S_6$ content exhibit rather dramatic changes. An intense narrow band emerges at 380 cm^{-1}, its position practically coinciding with the most intense Raman band of a $Sn_2P_2S_6$ crystal. There it corresponds to the stretching vibration of the P–P bond connecting two PS_3 pyramids in the $Sn_2P_2S_6$ structure [7]. Besides, the maxima at 142, 183, and 244 cm^{-1} become more intense and sharper, as well as new features appear at 65, 84, 110, 244, and 295 cm^{-1}. Note that the frequency positions of all these bands correlate with the known $Sn_2P_2S_6$ phonon spectrum [9] as well as with our earlier measurements for $Sn_2P_2S_6$ micro- and nanopowders and ceramics where features near 85, 140, 185, 245, 260, and 290 cm^{-1} were observed [22]. The observed features clearly confirm $Sn_2P_2S_6$ crystallite formation in the glass matrix under annealing.

Three distinct peaks at 340, 349, and 359 cm^{-1} appear on the background of the intense broad As_2S_3 glass-related maximum. Three bands with similar frequencies in this spectral range are characteristic for As_4S_4 structural groups [32]. Moreover, As_4S_4 structural groups can contribute to the weaker maxima observed near 140, 185, and 220 cm^{-1}, since features with similar frequencies are present in the realgar (As_4S_4) phonon spectrum [32]. Note that a similar effect of distinct relatively narrow As_4S_4-related peaks emerging on the

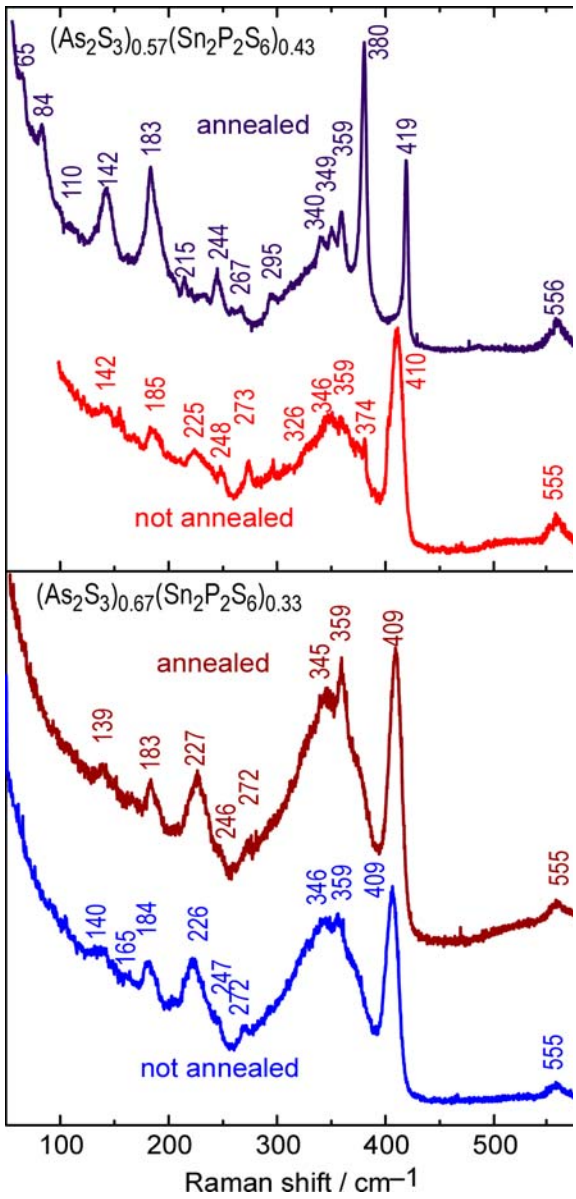

Fig. 5. Raman spectra of $(1–x)As_2S_3 \cdot xSn_2P_2S_6$ glasses before and after annealing at 573 K for 4 h.

background of the broad maximum near 350 cm^{-1} was observed with increasing As/S ratio from slightly substoichiometric (As-deficient) to slightly super-stoichiometric (S-deficient) arsenic sulphide glasses [41]. The authors conclude that even the stoichiometric glass can be separated into small As-rich (As_4S_4) and large S-rich clusters [41]. In our case, this can be evidence not only for the annealing-induced crystallization of $Sn_2P_2S_6$ from the Sn–As–P–S glass, but also the increasing clustering (phase separation) in the As_2S_3-based glass itself. Moreover, in view of the above quoted data of Ref. [39], the observed narrow bands emerging on the background of the broad maximum at 350 cm^{-1} correlate well with the decrease of sulphur content in the material after annealing as determined from the EDX data (Figs. 2 and 3).

It is also interesting that the relatively narrow band at 408 cm^{-1} ascribed to the breathing vibrations of distorted $As_2P_2S_4$ rings changes its frequency to the typical value of 418 cm^{-1}. This could mean that the annealing (and, possibly, the phase separation) results in a more stable As–P–S glass-like environment where the breathing vibrations of the $As_2P_2S_4$ rings occur with their usual frequency. Anyway, this is clear evidence for the fact that not all tin and phosphorus atoms participate in the $Sn_2P_2S_6$ crystallization and a considerable part of them is still kept within the Sn–As–P–S glass network.

4. Conclusions

Sn–As–P–S glasses were obtained by co-melting of As_2S_3 and $Sn_2P_2S_6$ in a broad compositional interval, their glass structure being clearly confirmed by micro-Raman spectra. SEM and EDX data show the evidence for phase transformations in the Sn–As–P–S samples annealed above 500 K, accompanied by a decrease of sulphur content with respect to the initial glass. Annealing-induced formation of $Sn_2P_2S_6$ crystallites is confirmed by Raman scattering data where sharp features, characteristic for $Sn_2P_2S_6$, are observed for the annealed samples with $Sn_2P_2S_6$ concentration $x > 0.4$. Sample heating induced by laser beam irradiation does not result in $Sn_2P_2S_6$ crystallization in the glass.

Acknowledgements

Yu.M. Azhniuk is grateful to Deutscher Akademischer Austauschdienst (DAAD) for the support of his research at Chemnitz University of Technology.

References

1. Yu. M. Vysochanskii, V.Yu. Slivka, Lifshitz point on the state diagram of ferroelectrics // *Sov. Phys. – Uspekhi,* **35**, p. 123-134 (1992).
2. J. Hlinka, T. Janssen, V. Dvořák, Order–disorder versus soft mode behaviour of the ferroelectric phase transition in $Sn_2P_2S_6$ // *J. Phys.: Condens. Matter*, **11**, p. 3209-3216 (1999).
3. M.B. Smirnov, J. Hlinka, A.V. Solov'ev, Lattice dynamics and the ferroelectric phase transition in $Sn_2P_2S_6$ // *Phys. Rev. B*, **61**, p. 15051-15060 (2000).
4. S. Farahi, G. Montemezzani, A. A. Grabar, J.-P. Huignard, F. Ramaz, Photorefractive acousto-optic imaging in thick scattering media at 790 nm with a $Sn_2P_2S_6$:Te crystal // *Opt. Lett.* **35**, p. 1798-1800 (2010).
5. G. Dittmar, H. Schäfer, Die Struktur des Di-Zinn-Hexathiohypodiphosphats $Sn_2P_2S_6$ // *Z. Naturforsch. B*, **29**, p. 312-317 (1974).
6. M.M. Maior, Dielectric properties of $Sn_2P_2S_6$ crystals depending on the conditions of their fabrication // *Sov. Phys. Solid State*, **41**, p. 1333-1338 (1999).

7. Yu.M. Vysochanskii, V.Yu. Slivka, Yu.V. Voroshilov, M.I. Gurzan, D.V. Chepur, Polarization spectra of Raman scattering for $Sn_2P_2S_6$ ferrosemiconductor // *Sov. Phys. Solid. State*, **21**, p. 123-127 (1979).
8. A.V. Gomonnai, Yu.M. Vysochanskii, A.A. Grabar, V.Yu. Slivka, Anisotropy of Raman scattering spectra in $Sn_2P_2S_6$ // *Sov. Phys. Solid. State*, **23**, p. 2105-2109 (1981).
9. J. Hlinka, I. Gregora, V. Vorlíček, Complete spectrum of long-wavelength phonon modes in $Sn_2P_2S_6$ by Raman scattering // *Phys. Rev. B*, **65**, p. 064308-1–064308-9 (2002).
10. S.W.H. Eijt, R. Currat, J.E. Lorenzo, P. Saint-Grégoire, B. Hennion, Yu.M. Vysochanskii, Soft modes and phonon interactions in $Sn_2P_2S_6$ studied by inelastic neutron scattering // *Eur. J. Phys. B*, **5**, p. 169-178 (1998).
11. V. Samulionis, J. Banys, Yu. Vysochanskii, A. Grabar, The critical behavior of ultrasonic velocity at a second order phase transition in $Sn_2P_2S_6$ single crystals // *Phys. Status Solidi B*, **215**, p. 1151-1156 (1999).
12. I.P. Studenyak, V.V. Mitrovcij, Gy.Sh. Kovacs, O.A. Mykajlo, M.I. Gurzan, Yu.M. Vysochanskii, Temperature variation of optical absorption edge in $Sn_2P_2S_6$ and $Sn_2P_2Se_6$ crystals // *Ferroelectrics*, **254**, p. 295-310 (2001).
13. Yu.M. Vysochanskii, V.V. Mitrovcij, A.A. Grabar, S.I. Perechinskii, S.F. Motrja, J. Kroupa, Birefringence investigation of the $Sn_2P_2(Se_xS_{1-x})_6$ uniaxial ferroelectrics behaviour near the Lifshitz point // *Ferroelectrics*, **237**, p. 193-200 (2000).
14. D. Baltrunas, A.A. Grabar, K. Mazeika, Yu.M. Vysochanskii, Temperature investigations of ferroelectric crystals $Sn_2P_2S_6$ and $Sn_2P_2Se_6$ by means of ^{119}Sn Mossbauer spectroscopy // *J. Phys.: Condens. Matter*, **11**, p. 2983-2993 (1999).
15. Yu.M. Vysochanskii, D. Baltrunas, A.A. Grabar, K. Mazeika, K. Fedyo, A. Sudavicius, Mössbauer ^{119}Sn and XPS spectroscopy of $Sn_2P_2S_6$ and SnP_2S_6 crystals // *phys. status solidi* (*b*), **246**, p. 1110-1115 (2009).
16. K. Kuepper, B. Schneider, V. Caciuc, M. Neumann, A.V. Postnikov, A. Ruediger, A.A. Grabar, Yu.M. Vysochanskii, Electronic structure of $Sn_2P_2S_6$ // *Phys. Rev. B*, **67**, p. 115101-1–115101-7 (2003).
17. J. Grigas, E. Talik, V. Lazauskas, Yu.M. Vysochanskii, R.Yevych, M. Adamiec, V. Nelkinas, XPS of electronic structure of ferroelectric $Sn_2P_2S_6$ crystals // *Ferroelectrics*, **378**, p. 70-78 (2009).
18. A. Say, O. Mys, A.A. Grabar, Yu.M. Vysochanskii, R.O. Vlokh, Thermal expansion of $Sn_2P_2S_6$ // *Phase Transitions*, **82**, p. 531-540 (2009).
19. Y.W. Cho, S.K. Choi, Yu. M. Vysochanskii, Photovoltaic effect of $Sn_2P_2S_6$ crystal and ceramics // *J. Mater. Res.*, **16**, p. 3317-3322 (2001).
20. X. Bourdon, E. Prouzet, V.B. Cajipe, Room-temperature synthesis of $Sn_2P_2S_6$ // *J. Sol.-State Chem.* **129**, p. 157-159 (1997).
21. X. Bourdon, V.B. Cajipe, Soft-chemistry forms of $Sn_2P_2S_6$ and $CuInP_2S_6$ // *J. Sol.-State Chem.* **141**, p. 290-293 (1998).
22. A.V.Gomonnai, Yu.M.Azhniuk, Yu.M.Vysochanskii, A.A. Kikineshi, M. Kis-Varga, L. Daroczy, I.P. Prits, I.M. Voynarovych, Raman and X-ray diffraction studies of nanometric $Sn_2P_2S_6$ crystals // *J. Phys.: Condens. Matter*, **15**, p. 6381-6393 (2003).
23. M. Gasqnier, H. Szwarc, A. Petit, Synthesis of ditin hexathiophosphate $Sn_2P_2S_6$ by low-energy ball-milling and monomode microwave // *Mater. Res. Bull.* **38**, p. 1681-1694 (2003).
24. U. Woggon, *Optical Properties of Semiconductor Quantum Dots*, Springer, Berlin/Heidelberg, 1997.
25. Yu.M. Azhniuk, V.V. Lopushansky, A.V. Gomonnai, V.O. Yukhymchuk, I.I. Turok, Ya.I. Studenyak, Spectroscopic studies of thermal treatment effect on the composition and size of $CdS_{1-x}Se_x$ nanocrystals in borosilicate glass // *J. Phys. Chem. Sol.* **69**, p. 139-146 (2008).
26. Yu.M. Azhniuk, P. Bhandiwad, V.M. Rubish, P.P. Guranich, O.G. Guranich, A.V. Gomonnai, D.R.T. Zahn, Photoinduced changes in the structure of As_2S_3-based SbSI nanocrystal-containing composites studied by Raman spectroscopy // *Ferroelectrics*, **416**, p. 113-118 (2011).
27. Yu.M. Azhniuk, V. Stoyka, I. Petryshynets, V.M. Rubish, O.G. Guranich, A.V. Gomonnai, D.R.T. Zahn, SbSI nanocrystal formation in As–Sb–S–I glass under laser beam // *Mater. Res. Bull.* **47**, p. 1520-1522 (2012).
28. G. Lucovsky, Optic modes in amorphous As_2S_3 and As_2Se_3 // *Phys. Rev. B*, **6**, p. 1480-1489 (1972).
29. H. Kawamura, K. Fukumasu, Y. Hamada, Low-frequency inelastic light scattering from As–S glasses // *Solid State Communs.* **43**, p. 229-231 (1982).
30. T. Mori, K. Matsuishi, T. Arai, Vibrational properties and network topology of amorphous As–S systems // *J. Non-Cryst. Solids*, **65**, p. 269-283 (1984).
31. S. Mamedov, A. Bolotov, L. Brinker, A. Kisliuk, M. Soltwisch, M. Vlček, A. Sklenar, X-ray small-angle and Raman scattering from glasses in the As_2S_3–CuI system // *Phys. Rev. B*, **58**, p. 8155-8158 (1998).
32. M. Frumar, Z. Polák, Z. Černošek, Raman spectra and photostructural changes in the short-range order of amorphous As–S chalcogenides // *J. Non-Cryst. Solids*, **256–257**, p. 105-110 (1999).
33. M.S. Iovu, S.D. Shutov, A.M. Andriesh et al., Spectroscopic study of As_2S_3 glasses doped with Dy, Sm and Mn // *J. Non-Cryst. Solids*, **326–327**, p. 306-310 (2003).

34. N.V. Surovtsev, A.M. Pugachev, B.G. Nenashev, V.K. Malinovsky, Low-frequency Raman scattering in As_2S_3 glass former around the liquid–glass transition // *J. Phys.: Condens. Matter*, **15**, p. 7651-7662 (2003).
35. I. Ivan, M. Veres, I. Pócsik, S. Kokenyesi, Structural and optical changes in As_2S_3 thin films induced by light ion irradiation // *phys. status solidi* (*a*), **201**, p. 3193-3199 (2004).
36. K.S. Andrikopoulos, D. Christofilos, G.A. Kourouklis, and S.N. Yannopoulos, Pressure dependence of the Boson peak in glassy As_2S_3 studied by Raman Scattering // *J. Non-Cryst. Solids*, **352**, p. 4594-4600 (2006).
37. V.K. Tikhomirov, M. Barj, S. Turrell et al., Non-linear Raman effects and photodarkening in chalcogenide glass As_2S_3 // *Europhys. Lett.* **76**, p. 312-317 (2006).
38. L. Koudelka, M. Pisárčik, L.N. Blinov, M.S. Gutenev, Vibrational spectra and structure of As–P–S glasses // *J. Non-Cryst. Solids*, **134**, p. 86-93 (1991).
39. V.V. Shchennikov, N.V. Morozova, I. Tyagur, Yu. Tyagur, S.V. Ovsyannikov, Colossal tuning of an energy gap in $Sn_2P_2S_6$ under pressure // *Appl. Phys. Lett.* **99**, p. 212104-1–212104-3 (2011).
40. Yu.M. Azhniuk, A.V. Gomonnai, V.M Rubish, M.Yu. Rigan, O.O. Gomonnai, O.G. Guranich, D.R.T. Zahn, In situ Raman observation of laser-induced formation of $TlInSe_2$ crystallites in Tl–In–As–Se glass // *J. Phys. Chem. Solids*, **74**, p. 1452-1458 (2013).
41. D.D. Georgiev, P. Boolchand, K.A. Jackson, Intrinsic nanoscale phase separation of bulk As_2S_3 glass // *Phil. Mag.* **83**, p. 2941-2953 (2003).